Long non-coding RNA SNHG16 inhibits the oxygen-glucose deprivation and reoxygenation-induced apoptosis in human brain microvascular endothelial cells by regulating miR-15a-5p/bcl-2

HONGWEI TENG[1*], MING LI[2*], LEI QIAN[2], HUA YANG[1] and MINGZHI PANG[3]

Departments of [1]Neurosurgery and [2]Laboratory Medicine, Binhai County People's Hospital,
Yancheng, Jiangsu 224500; [3]Department of Neurosurgery, Wuxi No. 2 Hospital Affiliated
to Nanjing Medical University, Wuxi, Jiangsu 214002, P.R. China

Abstract. MicroRNA (miR) 15a-5p can promote ischemia/reperfusion (I/R)-induced apoptosis of cerebral vascular endothelial cells, which is inhibited by long non-coding RNAs (lncRNAs). The present study investigated the potential of lncRNAs targeting miR-15a-5p to regulate oxygen-glucose deprivation and reoxygenation (OGD-R)-induced apoptosis of human brain microvascular endothelial cells (hBMECs). hBMECs were transfected with or without miR-15a-5p or its mutant, together with p-small nucleolar RNA host gene 16 (SNHG16) or its mutant. Following OGD-R, proliferation, apoptosis and miR-15a-5p, SNHG16 and Bcl-2 expression levels were determined using MTT, flow cytometry, reverse transcription-quantitative PCR or western blotting. The potential interaction of SNHG16 with miR-15a-5p was analyzed by pull-down, luciferase and immunoprecipitation assays. OGD-R induced apoptosis of hBMECs and increased miR-15a-5p expression levels in a time-dependent manner. miR-15a-5p overexpression decreased the proliferation of hBMECs and promoted apoptosis by decreasing Bcl-2 expression levels. SNHG16 was pulled-down by miR-15a-5p and anti-Ago2. miR-15a-5p overexpression significantly decreased SNHG16-regulated luciferase activity and hBMEC survival by increasing apoptosis. SNHG16 overexpression decreased miR-15a-5p expression levels in hBMECs. SNHG16 gradually decreased following OGD-R and its overexpression decreased miR-15a-5p expression levels and promoted the proliferation of hBMECs by decreasing apoptosis. SNHG16 enhanced Bcl-2 expression levels in hBMECs, which was abrogated by miR-15a-5p. Bioinformatics suggest that SNHG16 may antagonize the binding of miR-15a-5p to the 3'UTR of Bcl-2 mRNA. These findings suggest that SNHG16 may protect hBMECs from OGD-R-induced apoptosis by antagonizing the miR-15a-5p/bcl-2 axis. Thus, targeting SNHG16-based mechanisms may provide novel therapeutic strategies for treatment of ischemic stroke.

Introduction

Ischemic stroke is the most common type of brain disease in adults worldwide; it is characterized by high incidence, disability and mortality rates (1). In China, the number of stroke-associated deaths has notably increased over the past two decades (1,2). Although rapid recanalization of the relevant artery and subsequent promotion of brain revascularization can successfully treat patients, reperfusion can increase the production of reactive oxygen species (ROS), inflammation and endoplasmic reticulum stress, leading to ischemia-reperfusion (I/R) injury, such as human brain microvascular endothelial cell (hBMEC) apoptosis (3). hBMECs, located between the blood and the brain parenchyma, are essential for normal neurological function and are responsible for transferring essential nutrients and removing potentially harmful toxins (4). I/R injury-induced hBMEC apoptosis impairs the therapeutic effect of relevant artery recanalization (5-7). Thus, protection of hBMECs from I/R injury may be crucial for intervention of ischemic stroke.

MicroRNAs (miR) can bind to the 3' untranslated region (3'UTR) of mRNAs, and inhibit their translation and promote their degradation, regulating a number of biological processes (8). For example, there is evidence to indicate that miR-15a-5p is involved in the pathogenesis of vascular endothelial cell injury following I/R (9). Induction of miR-15a-5p overexpression inhibits vascularization in a mouse model

Correspondence to: Dr Mingzhi Pang, Department of Neurosurgery, Wuxi No. 2 Hospital Affiliated to Nanjing Medical University, 68 Zhongshan Road, Chongan, Wuxi, Jiangsu 214002, P.R. China
E-mail: qianleiyc@163.com

*Contributed equally

of hind limb ischemia (9). Furthermore, increased levels of miR-15a-5p are detected in the heart following myocardial infarction, and inhibition of miR-15a-5p decreases infarct size and enhances cardiac function in mice that have experienced myocardial infarction (10). Notably, miR-15a-5p can decrease Bcl-2 expression levels and increase apoptosis of cerebral vascular endothelial cells following oxygen-glucose deprivation and reoxygenation (OGD-R) (11). However, little is currently known about which factors regulate miR-15a-5p expression levels following OGD-R in hBMECs.

Long non-coding RNAs (lncRNAs) are defined as being >200 nucleotides in length and function as miR sponges to regulate numerous biological processes, including apoptosis, inflammation and I/R injury (12,13). For example, expression levels of antisense non-coding RNA in the INK4 locus (ANRIL) are upregulated in the cortex in a rat model of cerebral infarction and ANRIL can activate the NF-κB signaling pathway to promote inflammation (12). The UCA1 lncRNA expression level is downregulated in myocardial tissues in a mouse model of I/R injury by targeting P27 to induce apoptosis (13). On the other hand, metastasis-associated lung adenocarcinoma transcript 1 (MALAT1) can target the pro-apoptotic protein Bim to decrease pro-inflammatory cytokine production in BMECs of mice with I/R-induced brain injury (14). The small nucleolar RNA host gene 16 (SNHG16) is a newly identified oncogenic lncRNA that regulates the progression and metastasis of lung, breast and bladder cancer (15,16). Previous studies have demonstrated that lncRNAs can share miRNA response elements (MREs) and induce gene silencing (17,18). However, it is currently unknown whether SNHG16 can interact with miR-15a-5p to regulate the proliferation and apoptosis of hBMECs during I/R.

The present study used hBMECs to investigate the effect of OGD-R on proliferation, apoptosis and miR-15a-5p, Bcl-2 and SNHG16 expression levels. The potential interaction of SNHG16 with miR-15a-5p was analyzed via pull-down, luciferase and immunoprecipitation assays.

Materials and methods

Establishment of an in vitro model of OGD-R. The hBMEC line hCMEC/D3 was obtained from Procell Life Science & Technology Co., Ltd. The cells were cultured in complete DMEM containing 10% fetal bovine serum (FBS; Gibco; Thermo Fisher Scientific, Inc.) for 24 h at 37°C in a humidified atmosphere of 5% CO_2. I/R injury of hBMECs was induced by OGD-R (19,20). Briefly, the cells were cultured in a medium without glucose and serum (Gibco; Thermo Fisher Scientific, Inc.) at 37°C in a 5% CO_2 and 95% N_2 hypoxic cell culture system (H35; Don Whitley Scientific) for 4 h and then cultured in complete medium at 37°C in 5% CO_2. hBMECs cultured in complete medium at 37°C in 5% CO_2 were used as the control.

Transfection with RNA oligoribonucleotides. The human SNHG16 wild-type or its mutant at (MREs) were cloned into the plasmid pmirGLO downstream of the Renilla luciferase open reading frame to generate the plasmid pSNHG16-wt or pSNHG16-mut (GenePharma), respectively. HBMECs were transfected with pSNHG16-wt or pSNHG16-mut, hsa-miR-15a-5p mimics or scrambled miRNA

(miR-NC; ON-TARGETplus SMARTpool; GE Healthcare Dharmacon, Inc.) at a final concentration of 100 nM using Lipofectamine® 2000 (Invitrogen; Thermo Fisher Scientific, Inc.) according to the manufacturer's recommendation. At 6 h post-transfection, the cells were subjected to OGD-R. The transfection efficiency in cells was determined using reverse transcription quantitative PCR (RT-qPCR).

Measurement of miR-15a-5p and SNHG16 using RT-qPCR. Total RNA was extracted from individual groups of hBMECs using TRIzol® reagent (Invitrogen; Thermo Fisher Scientific, Inc.) and reverse transcribed into cDNA at 50°C for 30 min using the cDNA Reverse Transcription kit (Applied Biosystems; Thermo Fisher Scientific, Inc.). The relative levels of target SNHG16 to control GAPDH mRNA transcripts were determined via RT-qPCR using SYBR Green (Thermo Fisher Scientific, Inc.) and specific primers in an Applied Biosystems 7500 PCR system (Applied Biosystems; Thermo Fisher Scientific, Inc.). The sequences of primers were: SNHG16: Forward 5'-CAGAATGCCATGGTTTCCCC-3'; reverse, 5'-TGGCAAGAGACTTCCTGAGG-3'; GAPDH: Forward, 5'-GCACCGTCAAGGCTGAGAAC-3'; reverse, 5'-ATGGT GGTGAAGACGCCA GT-3'. Similarly, the relative levels of miR-15a-5p to control U6 small nuclear RNA were analyzed using RT-qPCR using the TaqMan miRNA assay kit (Applied Biosystems; Thermo Fisher Scientific, Inc.). The thermocycling conditions were as follows: 20 sec at 95°C, followed by 40 cycles of 15 sec at 95°C and 60 sec at 60°C, and 60°C for 1 min. The data were normalized to the control and analyzed using the $2^{-\Delta\Delta Cq}$ method (21).

Cell apoptosis assay. The frequency of apoptotic hBMECs was determined by flow cytometry. Briefly, hBMECs ($1x10^5$ cells/well) were cultured in 10% FBS/DMEM (Gibco; Thermo Fisher Scientific, Inc.) for 24 h at 37°C in 5% CO_2 and subjected to OGD-R. Cells were collected at the indicated time points post-reoxygenation. The cells were stained with phycoerythrin-conjugated propidium iodide and FITC-conjugated Annexin V (both 1:10; both BD Biosciences) for 20 min at room temperature. The percentages of apoptotic cells were analyzed using a BD FACSCalibur flow cytometer (BD Biosciences).

Measurement of cell proliferation. Cell proliferation was measured using MTT assay. Briefly, hBMECs ($1x10^4$ cells/well) were cultured in 10% FBS/DMEM (Gibco; Thermo Fisher Scientific, Inc.) for 24 h at 37°C in 5% CO_2 and subjected to OGD-R. The cells were exposed to 10 μl of 5 mg/ml MTT for 4 h. The generated purple formazan in individual wells was dissolved in 50 μl DMSO. Absorbance was measured at 540 nm in a microplate reader (SpectraMax M5; Molecular Devices, LLC).

RNA-pull-down assay. hBMECs ($6x10^6$ cells) were cultured at 37°C for 24 h and were transfected with biotinylated miR-15a-5p, and scrambled miRNA (Guangzhou RiboBio Co., Ltd). After hBMECs were subjected to OGD-R, total RNAs were extracted at 48 h post-reoxygenation using the RNeasy Plus Mini kit (Qiagen GmbH) according to the manufacturer's instructions.. The biotinylated RNAs were absorbed with

Table I. Predicted miR-lncRNA interactions.

Gene	Target sites	bioComplex	clipReadNum	lncRNA relative expression level
SNHG16	1	9	185	22.6±2.1
CTBP1-AS1	1	1	27	7.3±1.6
RP11-869B15.1	1	2	19	1.1±0.3
RP11-169K16.9	1	1	12	3.2±0.6
RP11-384K6.6	1	1	19	2.6±1.4
AC074093.1	1	2	12	0.2±0.1
XIST	5	18	2,862	15.4±3.2
RP11-549J18.1	1	7	128	4.1±0.8
SENP3-EIF4A1	1	5	27	2.2±1.3
CTC-228N24.3	1	6	72	3.2±0.5
AC084219.4	2	10	193	14.6±2.9
LINC00094	1	8	143	3.7±2.8
RP11-403I13.4	2	4	46	7.9±1.4
ZNRD1-AS1	1	4	80	1.1±0.2
RP11-91G21.2	1	2	15	0.5±0.1
RP11-379K17.11	1	32	4,692	12.5±3.3
AC108142.1	1	2	11	0.3±0.1
MIR497HG	1	1	14	0.5±0.2
HCG17	1	2	25	2.3±0.3
RP13-507I23.1	1	1	72	3.2±0.4
C1RL-AS1	1	2	87	4.2±0.9
AP000721.4	1	9	233	7.3±2.3
RP11-96D1.10	1	1	51	6.6±1.7
ERVK13-1	1	1	25	5.3±1.1
RP3-341D10.4	1	2	17	1.5±0.2

Expression levels of lncRNA pulled-down by miR-15a-5p were detected using reverse transcription-quantitative PCR. The data were normalized to the control and analyzed using the $2^{-\Delta\Delta Cq}$ method. Data are expressed as the mean ± standard deviation of each group of cells from three separate experiments. miR, microRNA; lncRNA, long non-coding RNA.

M-280 streptaviden magnetic beads (Invitrogen; Thermo Fisher Scientific, Inc.) for 4 h at 4˚C. Next, the beads were washed with high salt buffer (1% Triton X-100; 0.1% SDS; 20 mM Tris-HCl, pH 8.0; 2 mM EDTA; 500 mM NaCl). The bound RNAs were measured using RT-qPCR as described above. Based on the starbase 2.0 analysis software (starbase.sysu.edu.cn/mirLncRNA.php), a total of 146 lncRNA that potentially formed complementary base pairs with miR-15a-5p (22). Among them, 25 lncRNAs were further analyzed according to their bioComplex and clipReadNum (Table I).

Isolation of cell cytoplasm/nucleus fractions. The cytoplasmic and nuclear components of individual groups of hBMECs were extracted using nuclear and cytoplasmic extraction reagents (Thermo Fisher Scientific, Inc.) according to the manufacturer's instructions. Briefly, $1x10^7$ cells re-suspended in 500 μl ice-cold cell fractionation buffer were incubated on ice for 10 min and centrifuged at 500 x g for 5 min at 4˚C. The cytoplasmic fraction in the supernatants was transferred into a new tube. The nuclear pellet was washed with ice-cold cell fractionation buffer and lysed in cell disruption buffer for RNA isolation. The extracted RNAs were analyzed using RT-qPCR as described above. The U6 and GAPDH were used as nuclear and cytoplasmic control transcripts, respectively.

RNA immunoprecipitation (RIP). RIP was performed using the Ago2 immunoprecipitation assay kit (Thermo Fisher Scientific, Inc.), according to the manufacturer's instructions. Briefly, hBMECs were lyzed in RIPA lysis buffer and centrifuged at 12,000 x g for 15 min at 4˚C. The supernatants were reacted with 10 μl beads and 2 μl argonaute 2 (Ago2) antibody or control IgG (1:100; cat. no. 17-700; EMD Millipore) rotating overnight at 4˚C. After being centrifuged at 12,000 x g for 15 min at 4˚C and washed with lysis buffer, RNAs were extracted using TRIzol® reagent and the presence of the binding targets was characterized by RT-qPCR as described above.

Dual luciferase reporter assay. In order to assess the SNHG16/miR-15a-5p binding specificity, luciferase activity was measured (Promega Corporation) according to the manufacturer's protocol. hBMECs were transfected in triplicate with 10 ug pSNHG16-wt or pSNHG16-mut, together with miR-15a-5p mimics or scrambled miRNA using
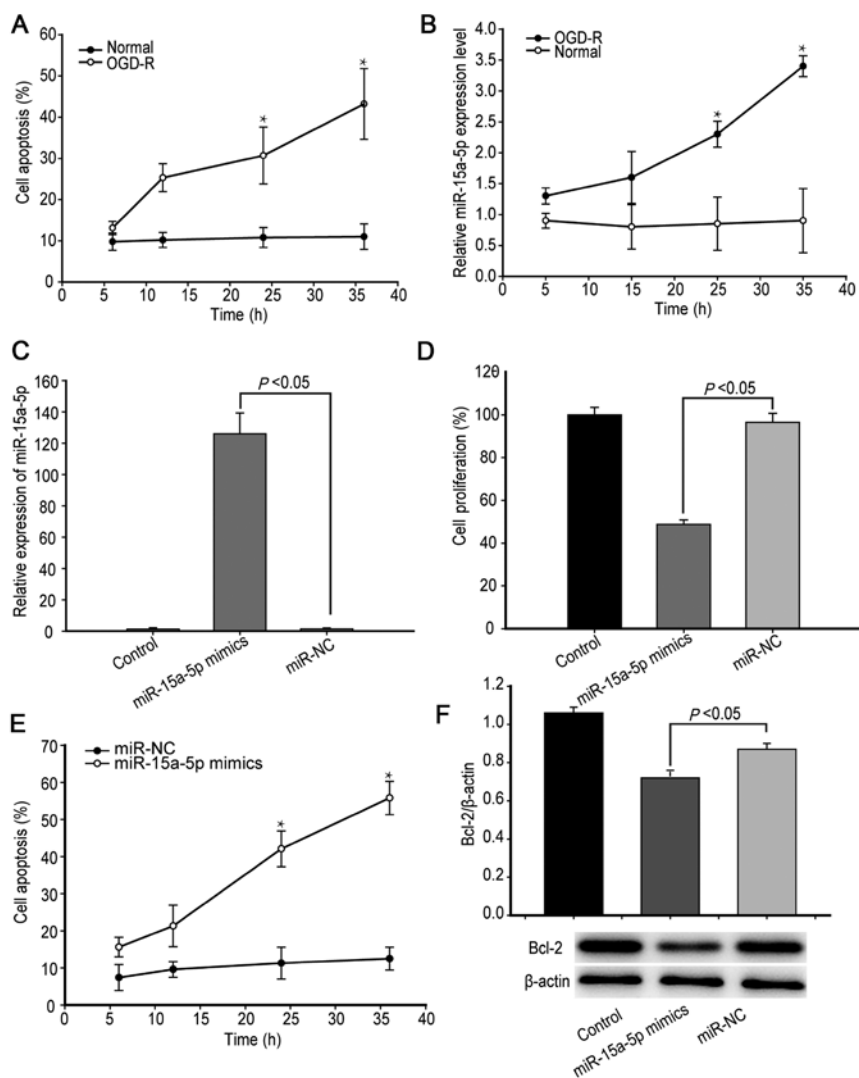
Figure 1. miR-15a-5p enhances OGD-R-induced apoptosis of hBMECs. (A) Percentages of apoptotic hBMECs were determined using flow cytometry at the indicated time points post-reoxygenation. Control cells were cultured under normal conditions. (B) Relative miR-15a-5p expression levels were measured using RT-qPCR. (C) Levels of miR-15a-5p in hBMECs were determined at 24 h post-transfection. (D) MTT analysis of cell proliferation at 48 h post-transfection. (E) Longitudinal analysis of apoptotic hBMECs using flow cytometry at 6, 12, 24 and 36 h. (F) Western blotting analysis of Bcl-2 expression levels at 48 h post-transfection. Statistical significance was analyzed by one-way analysis of variance followed by Tukey's multiple comparisons. Data are presented as the mean ± standard deviation of each group of cells from three separate experiments. *P<0.05. miR, microRNA; OGD-R, oxygen-glucose deprivation and reoxygenation; hBMEC, human brain microvascular endothelial cells; RT-qPCR, reverse transcription quantitative PCR; miR-NC, scrambled miR; WT, wild-type; MUT, mutant.

Lipofectamine® 2000. After transfection for 48 h, the relative luciferase activity in individual groups of cells was determined using a Lumat LB 9507 luminometer (Berthold Technologies; GmbH). The data were expressed as the fold change relative to the control groups defined as 1.0.

Western blotting. Individual groups of hBMECs were lyzed in RIPA lysis buffer (50 mM Tris-HCl, 1% Nonidet P-40, 150 mM NaCl, 0.5% sodium deoxycholate and 0.1% SDS) and centrifuged at 12,000 x g for 10 min at 4˚C. After the concentrations of total proteins were measured using a BCA protein assay kit (Pierce; Thermo Fisher Scientific, Inc.), individual samples (50 μg/lane) were analyzed using 10% SDS-PAGE and electrophoretically transferred onto PVDF membranes (EMD Millipore). After being blocked with 5% non-fat dry milk in Tris buffer saline with 0.1% Tween-20 (TBST) for 2 h at room temperature, the membranes were probed with anti-

bodies against Bcl-2 (1:100; cat. no. 15071) or β-actin (1:100; cat. no. 3700; all Cell Signaling Technology, Inc.) at 4˚C overnight. The bound antibodies were detected using horseradish peroxidase-conjugated anti-mouse IgG (1:200; cat. no. 7076; Cell Signaling Technology, Inc.) and visualized using the enhanced chemiluminescent reagents. The relative Bcl-2 to β-actin expression levels were determined using densitometric analysis using the Image Lab™ Software (version 3.0; Bio-Rad Laboratories, Inc.). A total of three independent experiments were performed.

Statistical analysis. Statistical analyses were performed using Stata 7.0 statistical software (StataCorp LP). The normal distribution of values was expressed as mean ± standard deviation and the difference among groups was analyzed by one-way analysis of variance followed by Tukey's multiple comparisons as a post-hoc test. The paired Student's t-tests was used to
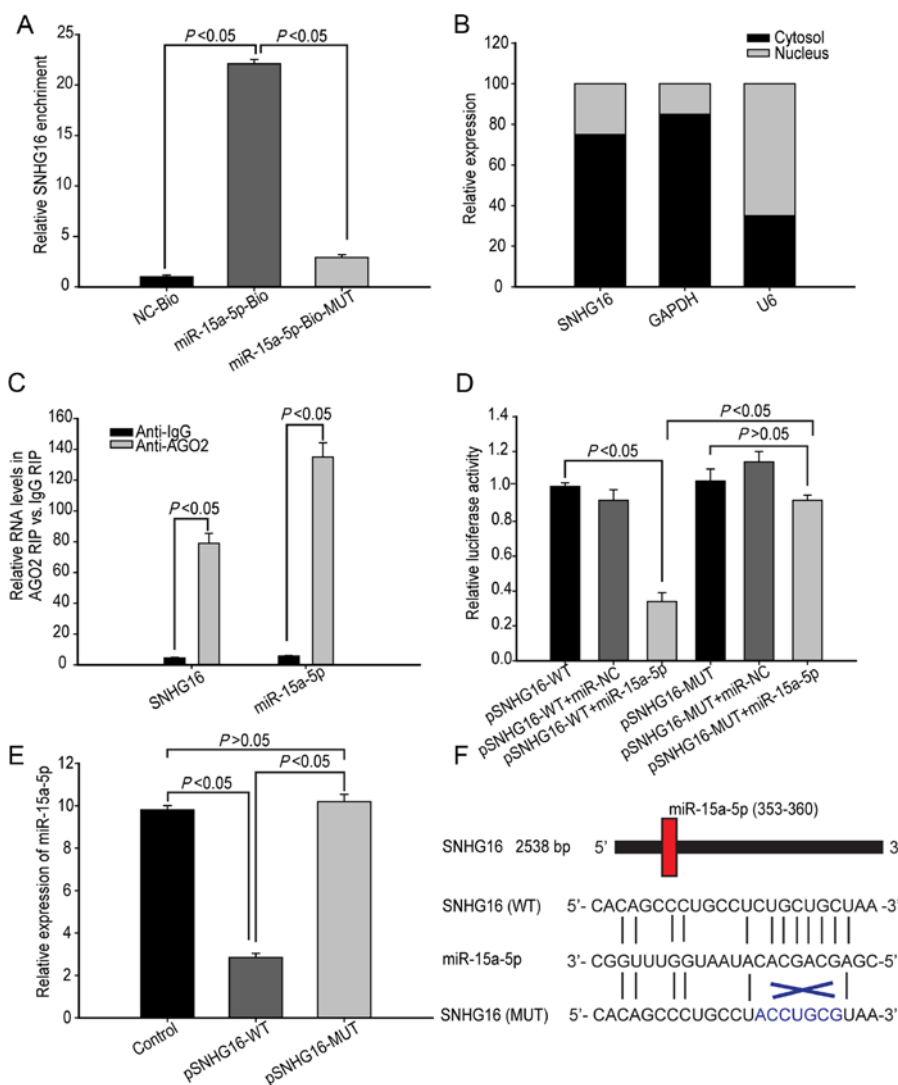
Figure 2. SNHG16 interacts with miR-15a-5p. hBMECs were subjected to OGD-R. At 48 h post-reoxygenation, the potential lncRNAs regulating miR-15a-5p were pulled down by miR-15a-5p and immunoprecipitated with anti-Ago2. (A) Levels of SNHG16 were pulled down using miR-15a-5p. (B) Cellular localization of SNHG16. (C) Immunoprecipitation analysis of SNHG16 and miR-15a-5p co-localization in Ago2 complex. (D) Luciferase assay demonstrated that miR-15a-5p decreased SNHG16-regulated luciferase activity in hBMECs. hBMECs were transfected with pSNHG16-wt or pSNHG16-mut together with miR-15a-5p or miR-NC under normal conditions for 24 h. Luciferase expression levels were determined using dual-luciferase assays. (E) SNHG16 overexpression downregulates miR-15a-5p expression levels in hBMECs at 48 h post-reoxygenation. (F) Predicted binding sites between SNHG16 and miR-15a-5p. Statistical significance was analyzed using one-way analysis of variance followed by Tukey's multiple comparisons. Data are presented as the mean ± standard deviation of each group of cells from three separate experiments. P<0.05. SNHG, small nucleolar host gene; miR, microRNA; hBMEC, human brain microvascular endothelial cells; OCD-R, oxygen-glucose deprivation and reoxygenation; lncRNA, long noncoding RNA; Ago2, argonaute 2; NC, normalized control.

compare percentages of apoptotic hBMECs and miR-15a-5p expression levels at the indicated time points. P<0.05 was considered to indicate a statistically significant difference.

Results

miR-15a-5p induces apoptosis of hBMECs. A previous study demonstrated that OGD-R can induce apoptosis of endothelial cells (23). In order to determine the effect of OGD-R on hBMECs in the present study, hBMECs were subjected to OGD-R or cultured in normal conditions, and the frequency of apoptotic hBMECs was determined using flow cytometry. The percentage of apoptotic hBMECs increased over the measured time points following OGD-R, whereas the percentage of control hBMECs undergoing apoptosis remained at ~10% throughout the experiment (Fig. 1A).

Analysis of miR-15a-5p expression levels indicated that the relative miR-15a-5p expression levels in hBMECs increased over time following OGD-R (Fig. 1B). In order to determine the role of miR-15a-5p, hBMECs were transfected with, or without, miR-15a-5p mimics or miR-NC for 24 h, and the relative levels of miR-15a-5p were determined using RT-qPCR. Transfection with miR-15a-5p mimics increased the levels of miR-15a-5p more than 120-fold (P<0.05; n=3; Fig. 1C). MTT and apoptosis assays demonstrated that increased miR-15a-5p expression levels significantly decreased the proliferation of hBMECs by triggering hBMEC apoptosis (P<0.05, Fig. 1D-E). As Bcl-2 is an important survival factor and a target of miR-15a-5p (11), the present study analyzed the relative Bcl-2 expression levels using western blotting. The results indicated that increased miR-15a-5p expression levels decreased Bcl-2 expression levels in hBMECs cultured in normal conditions
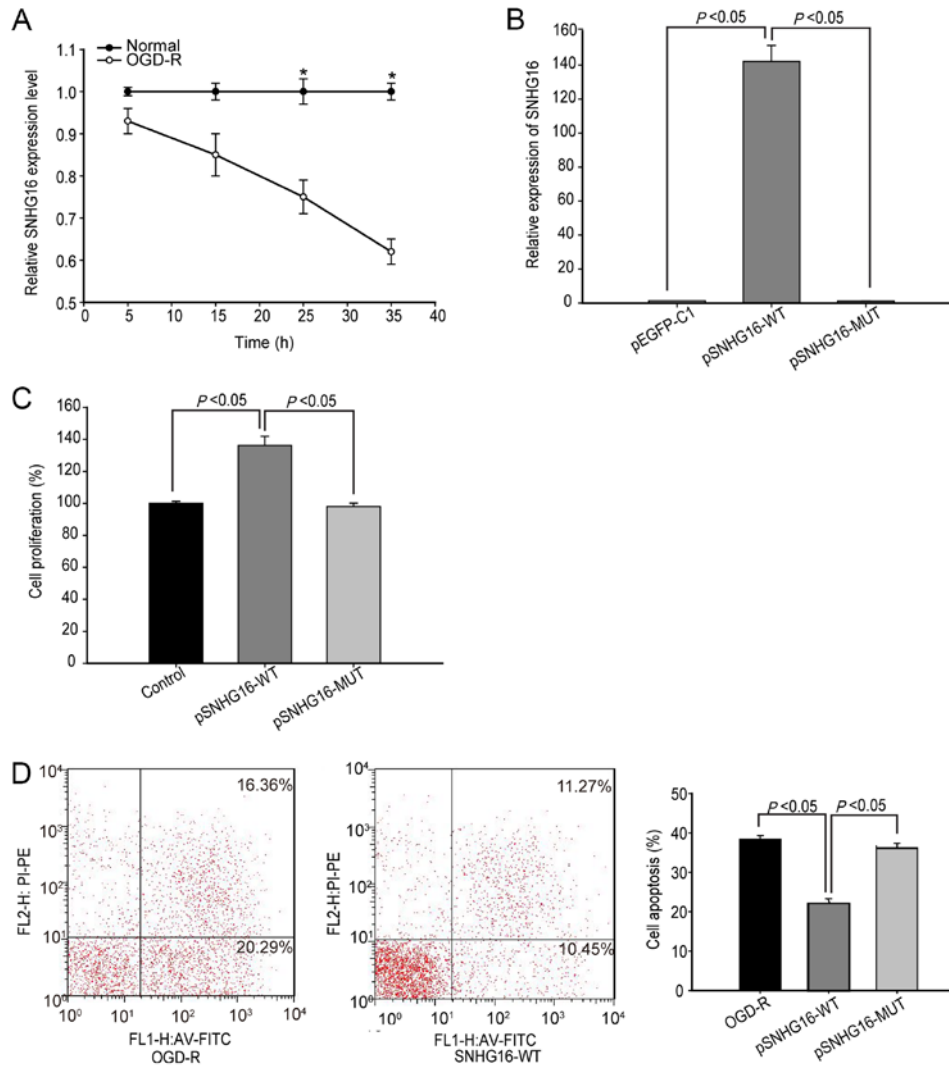
Figure 3. SNHG16 inhibits apoptosis of hBMECs. (A) OGD-R decreased SNHG16 expression levels in hBMECs. The levels of SNHG16 in the control cells cultured under normal conditions were designated as 1. (B) RT-qPCR analysis of SNHG16 expression in hBMECs at 24 h post-reoxygenation. (C) MTT analysis of SNHG16-enhanced proliferation of hBMECs at 48 h post-reoxygenation. (D) Flow cytometric analysis of SNHG16-decreased hBMEC apoptosis at 48 h post-reoxygenation. The lower right quadrant represents early apoptosis; the upper right quadrant represents late apoptosis. The rates of total apoptosis are presented as a bar plot. Statistical significance was analyzed using one-way analysis of variance followed by Tukey's multiple comparisons. Data are expressed as the mean ± standard deviation of each group of cells from three separate experiments. SNHG, small nucleolar host gene; hBMEC, human brain microvascular endothelial cells; OGD-R, oxygen-glucose deprivation and reoxygenation; RT-qPCR, reverse transcription quantitative PCR; WT, wild-type; MUT, mutant.

(P<0.05; Fig. 1F). The results of the present study indicated that OGD-R triggered hBMEC apoptosis by upregulating miR-15a-5p expression levels to decrease Bcl-2 expression levels.

SNHG16 regulates miR-15a-5p. lncRNAs can regulate miRNA expression levels. In order to screen potential lncRNAs that regulate miR-15a-5p expression levels, hBMECs were cultured under OGD-R for 48 h and potential RNAs were pulled-down. A total of 25 lncRNAs were identified, of which SNHG16 was the most abundant, as indicated by the results of RT-qPCR (Table I). SNHG16 was pulled-down by biotinylated miR-15a-5p, but not by the biotinylated miR-15a-5p mutant with a mutation at the binding site of SNHG16, indicating that SNHG16 interacted with miR-15a-5p (Fig. 2A). Therefore, SNHG16 was selected for subsequent experiments.

It was hypothesized that SNHG16 may act as a competitive endogenous RNA (ceRNA) in hBMECs by targeting miR-15a-5p. In order to test this, the cellular localization of SNHG16 was analyzed. As shown in Fig. 2B, SNHG16 was primarily distributed in the cytoplasm, suggesting that SNHG16 may play a role at a post-transcriptional level. As miRs are present in miR ribonucleoprotein complexes, which contain Ago2 protein, RIP was used to characterize SNHG16 distribution using anti-Ago2. The present study demonstrated that anti-Ago2 precipitated not only SNHG16, but also miR-15a-5p, suggesting that SNHG16 may be present in the miR-15a-5p RNA-induced silencing complex (Fig. 2C). Furthermore, luciferase reporter assays indicated that co-transfection with miR-15a-5p mimics, but not with control miR-NC, significantly decreased the luciferase activity of binding seed region in wild-type SNHG16 in hBMECs (P<0.05; n=3; Fig. 2D). However, miR-15a-5p mimics did not significantly affect the
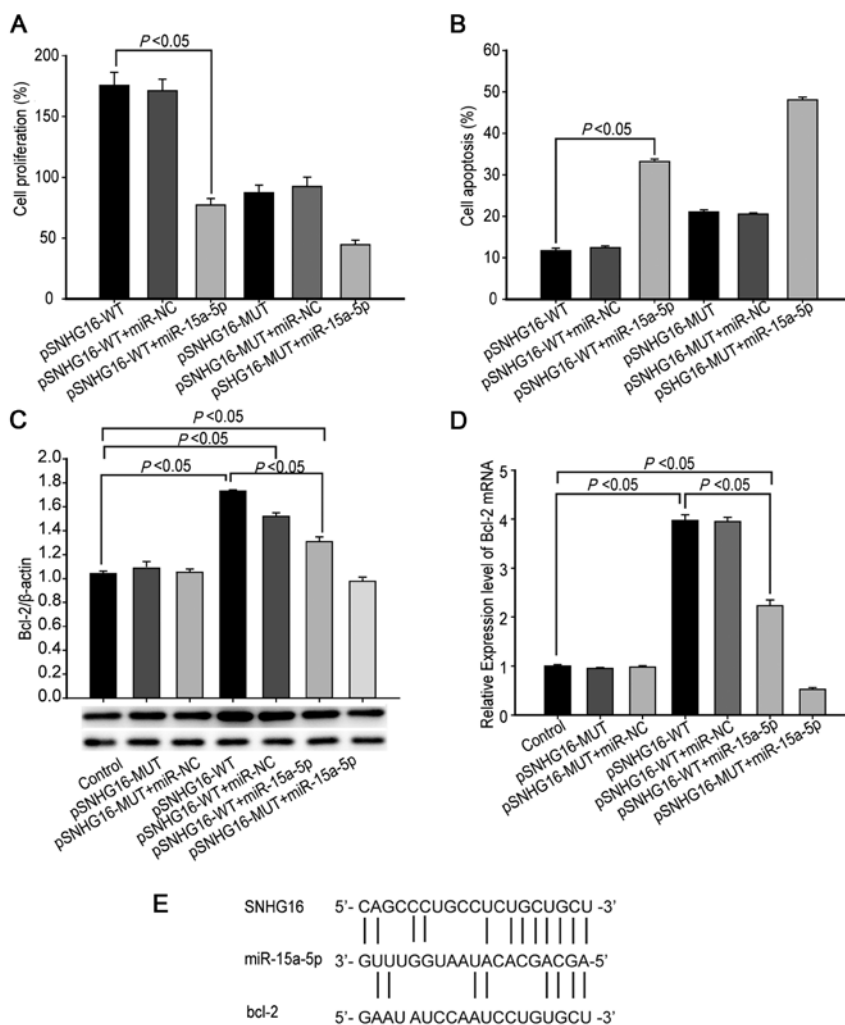
Figure 4. SNHG16 antagonizes miR-15a-5p to increase Bcl-2 expression levels and protect hBMECs from OGD-R-induced apoptosis. hBMECs were transfected with pSNHG16-wt or pSNHG16-mut, together with miR-15a-5p mimics or miR-NC and were subjected to OGD-R. At 48 h post-reoxygenation, the proliferation, apoptosis and Bcl-2 expression levels in hBMECs were determined. (A) MTT analysis of cell proliferation. (B) Flow cytometric analysis of cell apoptosis. (C) Western blotting analysis of Bcl-2 protein expression levels. (D) RT-qPCR analysis of Bcl-2 mRNA transcripts. (E) Potential binding sites among SNHG16, miR-15a-5p and Bcl-2 mRNA were predicted using bioinformatics using the online software starBase v2.0. SNHG16 may act as a molecular sponge for miR-15a-5p and regulate its target Bcl-2 expression levels. Statistical significance was analyzed by one-way analysis of variance followed by Tukey's multiple comparisons. Data are presented as the mean ± standard deviation of each group of cells from three separate experiments. SNHG, small nucleolar host gene; miR, microRNA; hBMEC, human brain microsvascular endothelial cell; OGD-R, oxygen-glucose deprivation and reoxygenation; NC, normalized control; RT-qPCR, reverse transcription quantitative PCR; WT, wild-type; MUT, mutant.

luciferase activity in mutant SNHG16 (P>0.05; n=3; Fig. 2D). Furthermore, overexpression of SNHG16, but not its mutant, significantly decreased the relative miR-15a-5p expression levels in hBMECs (P<0.05; n=3; Fig. 2E). Collectively, such data indicate that SNHG16 acts as a ceRNA to downregulate miR-15a-5p expression levels in hBMECs. The predicted binding sites of miR-15a-5p to SNHG16 and the coding sequence of SNHG16 at MREs are presented in Fig. 2F.

SNHG16 inhibits OGD-R induced apoptosis in hBMECs. The present study investigated the role of SNHG16 in regulating OGD-R induced apoptosis of hBMECs. Following reoxygenation, the relative level of SNHG16 transcripts in hBMECs gradually decreased compared with that in control cells cultured under normal conditions and reached 0.58-fold at 36 h post-reoxygenation (P<0.05; Fig. 3A). Furthermore, transfection with pSNHG16, but not its mutant, significantly increased SNHG16 expression levels and enhanced prolif-

eration of hBMECs at 48 h post-transfection (P<0.05; n=3; Fig. 3B and C). In accordance with these results, flow cytometric analysis indicated that transfection with pSNHG16, but not its mutant, significantly decreased the percentages of hBMECs undergoing OGD-R-induced apoptosis (36.3±1.5 vs. 21.1±1.9%; P<0.05; n=3; Fig. 3D). These results indicated that SNHG16 enhanced the proliferation of hBMECs and inhibited OGD-R-induced apoptosis.

SNHG16 inhibits miR-15a-5p-induced apoptosis in hBMECs. In order to further demonstrate the association between miR-15a-5p and SNHG16 in hBMECs, the present study determined whether SNHG16 could modulate the miR-15a-5p-regulated proliferation and apoptosis of hBMECs following OGD-R. HBMECs were co-transfected with pSNHG16-wt or pSNHG16-mut together with miR-15a-5p mimics or miR-NC and subjected to OGD-R. At 48 h post-reoxygenation, the proliferation of hBMECs was determined using MTT assay. Transfection with
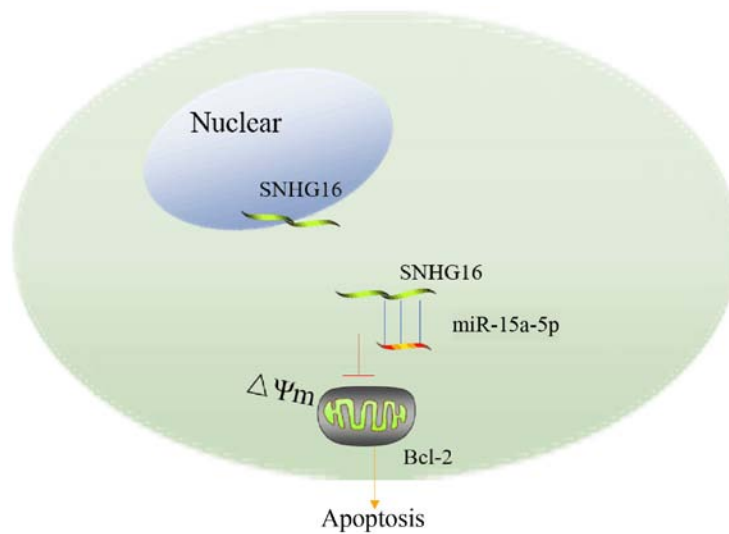
Figure 5. SNHG16/miR-15-5p/Bcl-2 axis. SNHG16 inhibits OGD-R-induced apoptosis in hBMEC by competitively sponging miR-15a-5p and regulating its target Bcl-2 expression levels. SNHG, small nucleolar host gene; miR, microRNA; OGD-R, oxygen-glucose deprivation and reoxygenation; hBMEC, human brain microvascular endothelial cells.

pSNHG16 and miR-NC significantly increased the proliferation of hBMECs, supporting the hypothesis that SNHG16 promotes hBMEC proliferation (P<0.05; n=3; Fig. 4A). In contrast, transfection with pSNHG16 and miR-15a-5p (both P<0.05, n=3) significantly decreased the proliferation of hBMECs (Fig. 4A). Similarly, transfection with miR-15a-5p significantly decreased the proliferation of SNHG16 mutant-overexpressing hBMECs. Flow cytometry indicated that transfection with miR-15a-5p significantly increased the percentages of apoptotic hBMECs that had been transfected with either pSNHG16 or pSNHG16 mutant (P<0.05; n=3; Fig. 4B). These results indicated that SNHG16 protects hBMECs from OGD-R-induced apoptosis by targeting miR-15a-5p.

SNHG16 positively regulates Bcl-2 expression levels in hBMECs. Bcl-2 is a regulator of cell survival and apoptosis and a potential target of miR-15a-5p (24). Accordingly, it was hypothesized that SNHG16 inhibited OGD-R-induced apoptosis by antagonizing miR-15a-5p to upregulate Bcl-2 in hBMECs. In order to investigate this, hBMECs were co-transfected with, or without, pSNHG16-wt or pSNHG16-mut together with miR-15a-5p mimics or miR-NC and subjected to OGD-R. At 48 h post-reoxygenation, the relative Bcl-2 expression levels in the different groups of cells were determined using western blotting and RT-qPCR. Transfection with either pSNHG16 mutant or together with miR-NC did not alter the relative levels of Bcl-2 expression in hBMECs, whereas transfection with pSNHG16 mutant and miR-15a-5p notably decreased Bcl-2 expression levels in hBMECs (P<0.05; n=3; Fig. 4C and D). Furthermore, transfection with pSNHG16 and miR-NC significantly increased the relative Bcl-2 expression levels while transfection with pSNHG16 and miR-15a-5p significantly decreased Bcl-2 expression levels in hBMECs, although their Bcl-2 expression levels were significantly higher than those of the control cells (P<0.05 for all). Bioinformatics demonstrated that SNHG16 could bind to miR-15a-5p, which could, in turn, bind to the 3'UTR sequence of Bcl-2 (Fig. 4E). Collectively, these data indicated that there is a regulatory

signaling pathway in which SNHG16 regulates Bcl-2 via competitively sponging miR-15a-5p (Fig. 5).

Discussion

The present study investigated the potential function and molecular mechanisms by which SNHG16 regulates OGD-R-induced apoptosis in hBMECs. The present study demonstrated that SNHG16 expression levels in hBMECs decreased in a time-dependent manner following OGD-R. Induction of SNHG16 overexpression significantly enhanced the proliferation of hBMECs by inhibiting OGD-R-induced apoptosis. The present study further demonstrated that SNHG16 directly interacted with miR-15a-5p to enhance Bcl-2 expression levels in hBMECs.

In previous studies, lncRNAs have been demonstrated to have a pivotal role in I/R injury. Microarray and RNA-seq techniques have identified a number of abnormally expressed lncRNAs in animal models of I/R injury and patients with ischemic stroke (25,26). Furthermore, certain lncRNAs have been demonstrated to regulate the pathogenesis of I/R injury. For example, MALAT1 protects hBMECs from OGD-R-induced apoptosis by enhancing PI3K dependent signaling (23). The present study demonstrated that OGD-R induced apoptosis in ~40% of hBMECs. Induction of SNHG16 overexpression significantly decreased the amount of apoptotic hBMECs following OGD-R. The results of the present study coincided with previous observations that SNHG16 promoted proliferation, migration and epithelial-to-mesenchymal transition in esophageal squamous cell carcinoma cells (27).

Gene expression levels can be modulated by lncRNA at epigenetic, transcriptional and post-transcriptional levels (28). In addition, a number of lncRNAs contain MREs and bind to certain miRNAs, acting as ceRNAs to decrease the functions of miRNAs at the post-transcriptional level (29). In order to screen potential lncRNAs that may serve as miR-15a-5p sponges, the present study used bioinformatics analysis and RNA-pull-down assay. The present study demonstrated that

SNHG16 was effectively pulled down by miR-15a-5p and was primarily located in the cytoplasm of hBMECs. Luciferase reporter assays demonstrated that miR-15a-5p can directly bind to SNHG16 via the putative MRE. Furthermore, induction of SNHG16 significantly decreased relative miR-15a-5p expression levels in hBMECs. RIP and dual luciferase reporter assays demonstrated that SNHG16 downregulated the function of miR-15a-5p by acting as a ceRNA.

Previous studies have demonstrated that miR-15a-5p regulates endothelial cell apoptosis during I/R injury (11,30). I/R-induced apoptosis of cardiomyocytes can be promoted by miR-15a-5p by targeting mothers against decapentaplegic homolog 7; inhibition of miR-15a-5p has the opposite effect (30). The present study demonstrated that miR-15a-5p expression levels increased in a time-dependent manner in hBMECs following OGD-R, which was consistent with previous reports (9,30). In addition, miR-15a-5p overexpression significantly decreased the proliferation of hBMECs by decreasing Bcl-2 expression levels. The results of the present study support the hypothesis that miR-15a-5p contributes to the pathogenesis of I/R injury by enhancing OGD-R-induced endothelial cell apoptosis through targeting of Bcl-2 expression levels.

The present study further determined an association between miR-15a-5p and SNHG16 in hBMECs proliferation and apoptosis. The results of the present study indicated that SNHG16 could modulate miR-15a-5p-regulated apoptosis of hBMECs following OGD-R and that overexpression of miR-15a-5p largely inhibited hBMEC proliferation upregulated by SNHG16. These results indicated that SNHG16 promotes hBMEC proliferation by inhibiting miR-15a-5p. In contrast to the effects of miR-15a-5p, SNHG16 overexpression significantly upregulated Bcl-2 expression levels in hBMECs following OGD-R. Furthermore, overexpression of miR-15a-5p notably reversed the expression levels of Bcl-2 in hBMECs upregulated by SNHG16. Accordingly, SNHG16 may act as a ceRNA to antagonize miR-15a-5p and decrease its inhibitory effect on Bcl-2 expression levels in hBMECs following OGD-R. The results of the present study support previous observations that endogenous SNHG16 competes with miR-140-5p and miR-98 to promote the development of esophageal squamous cell carcinoma and breast cancer (15,27).

The present study highlighted the significance of the association between SNHG16, miR-15a-5p and transcription factor Bcl-2 in the regulation of apoptosis in hBMECs. The results of the present study indicate that SNHG16 may inhibit I/R-induced apoptosis of hBMECs during cerebral I/R injury. Mechanistically, SNHG16 may serve as a molecular sponge to target miR-15a-5p and upregulate Bcl-2 expression levels. Thus, targeting SNHG16-based mechanisms may provide novel therapeutic strategies and aid in drug development for I/R injury.

Acknowledgements

Funding

Availability of data and materials

All data generated or analyzed during this study are included in this published article.

Authors' contributions

MP designed the study and drafted the manuscript. HT, ML, LQ, HY analyzed and interpreted the data. ML, LQ, HY performed the experiments. HT critically revised the manuscript. All authors read and approved the final manuscript.

Ethics approval and consent to participate

Not applicable.

Patient consent for publication

Not applicable.

Competing interests

The authors declare that they have no competing interests.

References

1. Zheng L, Cheng W, Wang X, Yang Z, Zhou X and Pan C: Overexpression of MicroRNA-145 ameliorates astrocyte injury by targeting aquaporin 4 in cerebral ischemic stroke. BioMed Res Int 2017: 9530951, 2017.
2. Poisson SN, Schardt TQ, Dingman A and Bernard TJ: Etiology and treatment of arterial ischemic stroke in children and young adults. Curr Treat Options Neurol 16: 315, 2014.
3. Emberson J, Lees KR, Lyden P, Blackwell L, Albers G, Bluhmki E, Brott T, Cohen G, Davis S, Donnan G, et al; Stroke Thrombolysis Trialists' Collaborative Group: Effect of treatment delay, age, and stroke severity on the effects of intravenous thrombolysis with alteplase for acute ischaemic stroke: A meta-analysis of individual patient data from randomised trials. Lancet 384: 1929-1935, 2014.
4. Alkabie S, Basivireddy J, Zhou L, Roskams J, Rieckmann P and Quandt JA: SPARC expression by cerebral microvascular endothelial cells in vitro and its influence on blood-brain barrier properties. J Neuroinflammation 13: 225, 2016.
5. Yang Q, He GW, Underwood MJ and Yu CM: Cellular and molecular mechanisms of endothelial ischemia/reperfusion injury: Perspectives and implications for postischemic myocardial protection. Am J Transl Res 8: 765-777, 2016.
6. Kong Q, Dai L, Wang Y, Zhang X, Li C, Jiang S, Li Y, Ding Z and Liu L: HSPA12B attenuated acute myocardial ischemia/reperfusion injury via maintaining endothelialIntegrity in a PI3K/Akt/mTOR-dependent mechanism. Sci Rep 6: 33636, 2016.
7. Sun ZY, Wang FJ, Guo H, Chen L, Chai LJ, Li RL, Hu LM, Wang H and Wang SX: Shuxuetong injection protects cerebral microvascular endothelial cells against oxygen-glucose deprivation reperfusion. Neural Regen Res 14: 783-793, 2019.
8. Suárez Y and Sessa WC: MicroRNAs as novel regulators of angiogenesis. Circ Res 104: 442-454, 2009.
9. Hullinger TG, Montgomery RL, Seto AG, Dickinson BA, Semus HM, Lynch JM, Dalby CM, Robinson K, Stack C, Latimer PA, et al: Inhibition of miR-15 protects against cardiac ischemic injury. Circ Res 110: 71-81, 2012.
10. Yin KJ, Olsen K, Hamblin M, Zhang J, Schwendeman SP and Chen YE: Vascular endothelial cell-specific microRNA-15a inhibits angiogenesis in hindlimb ischemia. J Biol Chem 287: 27055-27064, 2012.
11. Yin KJ, Deng Z, Hamblin M, Xiang Y, Huang H, Zhang J, Jiang X, Wang Y and Chen YE: Peroxisome proliferator-activated receptor delta regulation of miR-15a in ischemia-induced cerebral vascular endothelial injury. J Neurosci 30: 6398-6408, 2010.

12. Zhang B, Wang D, Ji TF, Shi L and Yu JL: Overexpression of lncRNA ANRIL up-regulates VEGF expression and promotes angiogenesis of diabetes mellitus combined with cerebral infarction by activating NF-κB signaling pathway in a rat model. Oncotarget 8: 17347-17359, 2017.
13. Liu Y, Zhou D, Li G, Ming X, Tu YF, Tian J, Lu H and Yu B: Long non coding RNA-UCA1 contributes to cardiomyocyte apoptosis by suppression of p27 expression. Cell Physiol Biochem 35: 1986-1998, 2015.
14. Zhang X, Tang X, Liu K, Hamblin MH and Yin KJ: Long noncoding RNA Malat1 regulates cerebrovascular pathologies in ischemic stroke. J Neurosci 37: 1797-1806, 2017.
15. Cai C, Huo Q, Wang X, Chen B and Yang Q: SNHG16 contributes to breast cancer cell migration by competitively binding miR-98 with E2F5. Biochem Biophys Res Commun 485: 272-278, 2017.
16. Christensen LL, True K, Hamilton MP, Nielsen MM, Damas ND, Damgaard CK, Ongen H, Dermitzakis E, Bramsen JB, Pedersen JS, *et al*: SNHG16 is regulated by the Wnt pathway in colorectal cancer and affects genes involved in lipid metabolism. Mol Oncol 10: 1266-1282, 2016.
17. Veneziano D, Marceca GP, Di Bella S, Nigita G, Distefano R and Croce CM: Investigating miRNA-lncRNA Interactions: Computational Tools and Resources. Methods Mol Biol 1970: 251-277, 2019.
18. Wang W, Lou W, Ding B, Yang B, Lu H, Kong Q and Fan W: A novel mRNA-miRNA-lncRNA competing endogenous RNA triple sub-network associated with prognosis of pancreatic cancer. Aging (Albany NY) 11: 2610-2627, 2019.
19. Wang J, Chen Y, Yang Y, Xiao X, Chen S, Zhang C, Jacobs B, Zhao B, Bihl J and Chen Y: Endothelial progenitor cells and neural progenitor cells synergistically protect cerebral endothelial cells from Hypoxia/reoxygenation-induced injury via activating the PI3K/Akt pathway. Mol Brain 9: 12, 2016.
20. Alluri H, Anasooya Shaji C, Davis ML and Tharakan B: Oxygen-glucose deprivation and reoxygenation as an in vitro ischemia-reperfusion injury model for studying blood-brain barrier dysfunction. J Vis Exp (99): e52699, 2015.
21. Livak KJ and Schmittgen TD: Analysis of relative gene expression data using real-time quantitative PCR and the 2(-Delta Delta C(T)) method. Methods 25: 402-408, 2001.
22. Li JH, Liu S, Zhou H, Qu LH and Yang JH: starBase v2.0: Decoding miRNA-ceRNA, miRNA-ncRNA and protein-RNA interaction networks from large-scale CLIP-Seq data. Nucleic Acids Res 42 (D1): D92-D97, 2014.
23. Xin JW and Jiang YG: Long noncoding RNA MALAT1 inhibits apoptosis induced by oxygen-glucose deprivation and reoxygenation in human brain microvascular endothelial cells. Exp Ther Med 13: 1225-1234, 2017.
24. Hao R, Hu X, Wu C and Li N: Hypoxia-induced miR-15a promotes mesenchymal ablation and adaptation to hypoxia during lung development in chicken. PLoS One 9: e98868, 2014.
25. Dykstra-Aiello C, Jickling GC, Ander BP, Shroff N, Zhan X, Liu D, Hull H, Orantia M, Stamova BS and Sharp FR: Altered expression of long noncoding RNAs in blood after ischemic stroke and proximity to putative stroke risk loci. Stroke 47: 2896-2903, 2016.
26. Zhang J, Yuan L, Zhang X, Hamblin MH, Zhu T, Meng F, Li Y, Chen YE and Yin KJ: Altered long non-coding RNA transcriptomic profiles in brain microvascular endothelium after cerebral ischemia. Exp Neurol 277: 162-170, 2016.
27. Zhang K, Chen J, Song H and Chen LB: SNHG16/miR-140-5p axis promotes esophagus cancer cell proliferation, migration and EMT formation through regulating ZEB1. Oncotarget 9: 1028-1040, 2017.
28. Ren W and Yang X: Pathophysiology of long non-coding RNAs in ischemic stroke. Front Mol Neurosci 11: 96, 2018.
29. Ebert MS, Neilson JR and Sharp PA: MicroRNA sponges: Competitive inhibitors of small RNAs in mammalian cells. Nat Methods 4: 721-726, 2007.
30. Yang Y, Ding S, Xu G, Chen F and Ding F: MicroRNA-15a inhibition protects against hypoxia/reoxygenation-induced apoptosis of cardiomyocytes by targeting mothers against decapentaplegic homolog 7. Mol Med Rep 15: 3699-3705, 2017.